DALTON
FULL PAPER

Hydrogen-bonded aggregates of protonated decavanadate anions in their tetraalkylammonium salts† ‡

Setsuko Nakamura and Tomoji Ozeki *

Department of Chemistry and Materials Science, Tokyo Institute of Technology, O-okayama, Meguro-ku, Tokyo 152-8551, Japan

Received 9th October 2000, Accepted 12th December 2000
First published as an Advance Article on the web 30th January 2001

Decavanadate anions with various degrees of protonation were crystallized with tetraalkylammonium cations, R_4N^+, where R represents CH_3, C_2H_5, *n*-C_3H_7, or *n*-C_4H_9. Structure analyses of seven such crystals reveal that these cations allow decavanadate anions to assemble with each other forming various kinds of hydrogen-bonded aggregates. Four types of assembly patterns have been observed: a diprotonated dimer, $([H_2V_{10}O_{28}]^{4-})_2$, two kinds of triprotonated dimers, $([H_3V_{10}O_{28}]^{3-})_2$, and a tetraprotonated polymer, $([H_4V_{10}O_{28}]^{2-})_\infty$. Among these, one of the triprotonated dimers exhibits an unprecedented assembly pattern. The degree of protonation in the solid state tends to increase as the size of the cation becomes larger. Each aggregate shows characteristic IR bands in the region 1000–400 cm^{-1}, from which the assembly patterns are distinguishable. The stabilization energies of the hydrogen-bonded aggregates are approximated well by the sum of the hydrogen-bond and electrostatic energies.

Introduction

Polyoxometalates[1] in the solid state have been attracting much attention in materials science[2] due to the richness in their structural, catalytic and magnetic properties. The development of new materials with novel properties requires the ability to arrange the constituent molecules or atoms in specific arrangements with appropriate intermolecular distances and orientations. It is thus essential to understand how the structure and properties of an individual molecule influence the resulting crystal, and how the molecules interact with each other in their crystalline state. In the past few decades a number of self-assembly patterns in molecular crystals of organic compounds have been studied from this point of view. Intermolecular interactions such as hydrogen bonds, S···S contacts and π–π stackings are found to be efficient means of organizing molecules into predictable arrangements in the crystalline state.[3] The synthons[4] for these interactions are readily distinguishable in the organic molecules, leading to the design of specific molecular arrangements in the crystalline state. For inorganic crystals with simple chemical compositions such as AX and AX_2, their crystal structures have been systematically investigated. It is known that these ionic compounds tend to crystallize so that each atom is coordinated by as many neighboring atoms as possible with the highest possible packing efficiency. Thus, crystal structures with the same stoichiometric index can be classified into different structure types, depending on the quotient of their ionic radii, r_A/r_X.

On the other hand, the guiding principles of the crystal structures of polyoxometalates are much less well understood. The fact that polyoxometalate anions have significant size and non-spherical shape distinguishes them from simple inorganic ions. In addition, some of the surface oxygen atoms can participate in intermolecular hydrogen bonds either as acceptors or donors, when they are unprotonated or protonated, respectively. Therefore, crystal structures of polyoxometalates can no longer approximate the close packing of spheres. Polyoxometalate solids are also different from organic solids in that the synthons of polyoxometalates, the hydrogen bond donor and acceptor sites, are not readily distinguishable. Of the oxygen atoms composing polyoxometalate surfaces, some accept hydrogen bonds and others do not; some protonate to become hydrogen bond donors and others do not. Moreover, some anions show various protonation and hydrogen bond acceptor sites depending on their environments in the crystals. Although the protons in the polyoxometalate crystals play important roles in defining their packing through hydrogen bonds, a systematic survey on the positions of the protons and the geometries of the hydrogen bonds is lacking. Only a limited number of structural investigations have been reported,[5,6] partly because the direct determination of the locations of the hydrogen atoms in polyoxometalate crystals by X-ray diffraction method requires data of sufficient quality.

Our objective is to find the key factors that determine the crystal structures of polyoxometalates, to develop a methodology for constructing arrays of polyoxometalate anions using non-covalent interactions, and then to design the crystal structures of these compounds. For this purpose, it is essential to investigate the protonation of polyoxometalate anions, the characteristics of hydrogen bonds of polyoxometalates, and the assembly patterns constructed by hydrogen bonding. In this study we employed decavanadate anions[7] with various degrees of protonation, $[H_nV_{10}O_{28}]^{(6-n)-}$ where $n = 2$, 3 or 4, as the target materials. The decavanadate anion, shown in Fig. 1, is a stable oxovanadate complex in acidic aqueous solutions and has been known, since the very early stage of polyoxometalate chemistry, to protonate in multiple steps depending on the acidity of the solution.[8] The protonation sites of this anion have been investigated widely both in solution by NMR[5,9] and in the solid state. X-Ray diffraction analyses of this anion with various inorganic[10] and organic[5,11–20] cations show that protonation in the crystalline state occurs mainly with organic cations. Protonation occurs only at a few particular surface oxygen sites: O(B) and O(C).[21] In the solid state, di-, tri- and tetraprotonated decavanadate anions have been observed, of which diprotonated ones show three types of protonation patterns. These include a centrosymmetric protonation at O(B1) and

† Dedicated to the memory of Dr H. T. Evans, Jr. (1920–2000).
‡ Electronic supplementary information (ESI) available: rotatable 3-D crystal structure diagrams in CHIME format. See http://www.rsc.org/suppdata/dt/b0/b008128k/

 DOI: 10.1039/b008128k

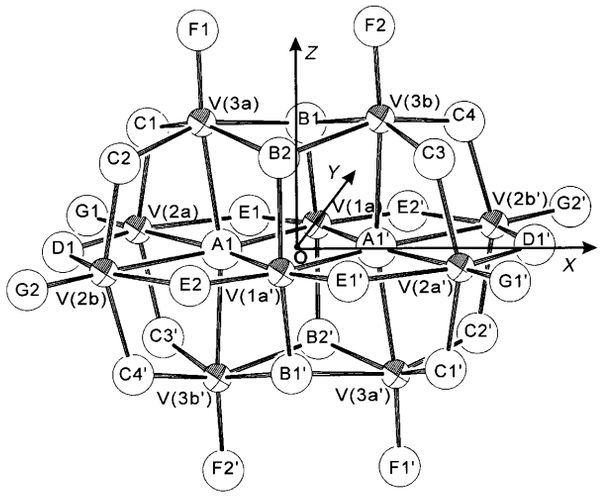

Fig. 1 Perspective view of the $[V_{10}O_{28}]^{6-}$ anion. The atom types are denoted following Day, *et al.*[5] The coordinate system is defined as the origin at the center of gravity and the three axes along the inertial axes of the configuration of the 10 V atoms. When the anion does not have a center of symmetry, labels with primes are used to designate the atoms related by the pseudoinversion center to the atoms labeled without primes.

O(B1′),[11,12] another centrosymmetric protonation at O(C1) and O(C1′),[12–15] and a non-symmetric protonation at O(B1) and O(C1).[15–17] The geometries of their hydrogen-bond networks show even more diversity. The triprotonated decavanadate anion has been found in $[(C_6H_5)_4P]^+$,[5] $[C_7H_{10}N]^+$ [18] and $[C_6H_8N]^+$ [19] salts, each of which has a distinctive hydrogen bond network. The tetraprotonated decavanadate anion has been found in a $[(n\text{-}C_4H_9)_4N]^+$ salt,[20] in which a hydrogen-bonded chain structure is observed. The complexity of the hydrogen bond patterns observed in these decavanadate crystals seems to be, at least partly, due to the organic cations involved in the hydrogen bonds as donors, acceptors, or both. Hydrogen bonds between the decavanadate anions and the organic cations obscure the mechanism of self-assembly of the protonated decavanadate anions.

In order to carry out a systematic survey on the crystal structures of decavanadate anions, we employed tetraalkylammonium cations, R_4N^+ where R stands for CH_3 to n-C_6H_{13}, since various sizes of ions are readily available. They are also advantageous because they will not act as hydrogen-bond donors or acceptors toward the protonated anions. Thus, hydrogen bond patterns intrinsic to the decavanadate anions are expected to appear in these salts. From crystal structure analyses of seven decavanadate crystals obtained from aqueous solutions with the pH ranging from 3 to 7, we found that di-, tri- and tetra-protonated anions form hydrogen-bonded aggregates. Although the larger cations, with R = n-C_5H_{11} or n-C_6H_{13}, did not give single crystals from the aqueous solutions, IR spectra of these polycrystalline salts were found to be helpful in identifying their hydrogen-bond patterns. In five of the seven crystals studied the protons were found from Fourier difference syntheses and their atomic parameters successfully refined, allowing the geometries of the surface O–H groups with respect to the decavanadate frameworks to be investigated. The stabilization energy upon forming the hydrogen-bonded aggregates of protonated anions was estimated as the sum of the hydrogen bond energies and the electrostatic interaction energies. This estimation proved to be valid as it reproduced the observed aggregation patterns. The results presented here demonstrate clearly that a series of tetraalkylammonium cations are advantageous tools to construct hydrogen-bonded arrays of protonated polyoxometalate anions.

Experimental

Reagents and general procedures

The following were purchased from commercial sources and used without further purification: 99% V_2O_5, 30% hydrogen peroxide aqueous solution, 15% $[(CH_3)_4N]OH$ aqueous solution, 20% $[(C_2H_5)_4N]OH$ aqueous solution, 10% $[(n\text{-}C_3H_7)_4N]$-OH aqueous solution, 10% $[(n\text{-}C_4H_9)_4N]OH$ aqueous solution, 95% $La(CH_3CO_2)_3{\cdot}nH_2O$, 90.0% $NaVO_3$, 60% nitric acid and methanol (Wako); 99.5% $Na_2H_2edta{\cdot}2H_2O$, 96% sodium hydroxide, 85% phosphoric acid (Koso); 98% $[(n\text{-}C_3H_7)_4N]Br$, 97% $[(n\text{-}C_5H_{11})_4N]Br$ and 96% $[(n\text{-}C_6H_{13})_4N]Br$ (Kanto). Infrared spectra were recorded on a JASCO FT/IR-350 Spectrometer (4600–400 cm^{-1}), with the crystalline compounds mixed with potassium bromide and pressed into transparent pellets. Elemental analyses for C, H and N were performed at our department, and analyses of V were carried out using a Rigaku JY-38S ICP emission spectrometer.

Syntheses

$[(CH_3)_4N]_4[H_2V_{10}O_{28}]{\cdot}3.8H_2O$ (TMAh). An aqueous decavanadic solution (0.008 M, 100 mL) was obtained by a reaction between 0.74 g of V_2O_5 and 30 mL of 30% H_2O_2 in water, following the procedure described by Jahr and Preuss.[22] This solution was adjusted to pH 5.0 with 14.7 mL of 0.32 M $[(CH_3)_4N]OH$ aqueous solution. Orange prism crystals (0.35 g) precipitated after two weeks. ν_{max}/cm^{-1} 960vs, 840s, 760m, 600m, 460m and 400m (Found: C, 14.42; H, 4.56; N, 4.00; V, 38.84. Calc. for $C_{16}H_{57.6}N_4O_{31.8}V_{10}$: C, 14.51; H, 4.38; N, 4.23; V, 38.46%).

$[(C_2H_5)_4N]_3[H_3V_{10}O_{28}]{\cdot}2H_2O$ (TEAh). The pH of a decavanadic aqueous solution (0.008 M, 500 mL) was adjusted to 4.5 with 34.3 mL of 0.13 M $[(C_2H_5)_4N]OH$ aqueous solution. After two weeks, yellow plate crystals (0.70 g) of **TEAh** were obtained. ν_{max}/cm^{-1} 990s, 975vs, 840s, 800m, 780m, 720w, 610m, 560w and 460w (Found: C, 21.08; H, 4.88; N, 2.89; V, 36.90. Calc. for $C_{24}H_{67}N_3O_{30}V_{10}$: C, 20.78; H, 4.87; N, 3.03; V, 36.72%).

$[(n\text{-}C_3H_7)_4N]_3[H_3V_{10}O_{28}]{\cdot}0.5H_2O$ (TPAh). *Method 1.* Sodium metavanadate, $NaVO_3$ (4.5 g), was dissolved in hot water at about 60 °C. After filtering, 5.5 mL of 1.7 M phosphoric acid were added, when the colorless solution changed to dark purple. The total amount of this solution was set to 50 mL with water and then its pH was adjusted to 5.5 by adding 6.2 mL of 1.4 M nitric acid. The reaction between the dark purple solution and 7 mL of 0.53 M $[(n\text{-}C_3H_7)_4N]Br$ aqueous solution yielded after two months yellow prism crystals suitable for single crystal X-ray diffraction. ν_{max}/cm^{-1} 990sh, 970vs, 940m, 840s, 800s, 770s, 720m, 610s, 550m, 510m and 460m.

Method 2. An aqueous decavanadic solution (0.004 M, 100 mL) was adjusted to pH 5.0 with 4.0 mL of 0.5 M sodium hydroxide solution. The reaction mixture was filtered and 10 mL of 0.04 M $[(n\text{-}C_3H_7)_4N]Br$ aqueous solution were added. After a week polycrystalline materials showing an identical IR absorption spectrum to those above were isolated (Found: C, 28.25; H, 5.82; N, 2.55; V, 32.46. Calc. for $C_{36}H_{88}N_3O_{28.5}V_{10}$: C, 28.29; H, 5.80; N, 2.75; V, 33.33%).

$[(n\text{-}C_3H_7)_4N]_3[H_3V_{10}O_{28}]$ (TPAv). $La(CH_3CO_2)_3{\cdot}nH_2O$ (0.14 g) and $Na_2H_2edta{\cdot}2H_2O$ (0.15 g) were dissolved in 10 mL of water, which was then added to 100 mL of 0.004 M aqueous decavanadic solution. After filtering, the pH was adjusted to 5.0 with 15 mL of 0.16 M $[(n\text{-}C_3H_7)_4N]OH$ aqueous solution. After two weeks yellow plate crystals were obtained. The addition of La^{3+} and $Na_2H_2edta{\cdot}2H_2O$ solution delayed the crystal growth and yielded crystals suitable for single crystal X-ray diffraction. ν_{max}/cm^{-1} 990s, 970vs, 950s, 840s, 760m, 720m, 610m and

450m (Found: C, 28.68; H, 5.94; N, 2.62; V, 33.58. Calc. for $C_{36}H_{87}N_3O_{28}V_{10}$: C, 28.46; H, 5.77; N, 2.77; V, 33.53%).

$[(n\text{-}C_3H_7)_4N]_2[H_4V_{10}O_{28}]$ (TPAc). An aqueous decavanadic solution (0.004 M, 100 mL) was adjusted to pH 4.5 with 3.6 mL of 0.5 M sodium hydroxide solution. The reaction mixture was filtered and 10 mL of 0.14 M $[(n\text{-}C_3H_7)_4N]Br$ aqueous solution were added. After three weeks yellow needle crystals (0.08 g) were isolated. ν_{max}/cm^{-1} 990s, 980vs, 960s, 850s, 780s, 750s, 730sh, 620m, 580s and 440s (Found: C, 21.91; H, 4.65; N, 1.98; V, 38.72. Calc. for $C_{12}H_{30}NO_{14}V_5$: C, 21.61; H, 4.53; N, 2.10; V, 38.18%).

$[(n\text{-}C_4H_9)_4N]_3[H_3V_{10}O_{28}]$ (TBAh). The pH of a mixture of 0.004 M decavanadic solution (100 mL) and the La^{3+}–$Na_2H_2edta\cdot 2H_2O$ solution prepared as above (10 mL) was brought to 5.0 with 20.5 mL of 0.16 M $[(n\text{-}C_4H_9)_4N]OH$ aqueous solution. After a week orange prism crystals (0.14 g) precipitated. ν_{max}/cm^{-1} 990sh, 970vs, 950sh, 880w, 840s, 810s, 770s, 720m, 610s, 550m, 510w, 460m and 440w (Found: C, 34.40; H, 6.68; N, 2.36; V, 30.15. Calc. for $C_{48}H_{111}N_3O_{28}V_{10}$: C, 34.16; H, 6.63; N, 2.49; V, 30.18%).

$[(n\text{-}C_4H_9)_4N]_2[H_4V_{10}O_{28}]$ (TBAc). The reaction mixture prepared by dissolution of 0.28 g of $La(CH_3CO_2)_3\cdot nH_2O$ and 0.30 g of $[H_2edta]Na_2\cdot 2H_2O$ in 10 mL of water was added to 100 mL of 0.004 M aqueous decavanadic solution. The solution was adjusted to pH 3.5 with 7.5 mL of 0.16 M $[(n\text{-}C_4H_9)_4N]OH$ aqueous solution. After two days orange prism crystals (0.32 g) were obtained. ν_{max}/cm^{-1} 1000s, 990s, 960vs, 950sh, 850s, 780m, 760m, 620m, 580m, 560w and 450m (Found: C, 26.64; H, 5.36; N, 1.85; V, 35.20. Calc. for $C_{16}H_{38}NO_{14}V_5$: C, 26.57; H, 5.30; N, 1.94; V, 35.22%).

$[(n\text{-}C_5H_{11})_4N]_3[H_3V_{10}O_{28}]$. An aqueous solution containing 0.23 g of $[(n\text{-}C_5H_{11})_4N]Br$ (10 mL) was added to 50 mL of 0.004 M decavanadic aqueous solution. Polycrystalline compounds precipitated instantly (0.34 g). ν_{max}/cm^{-1} 990s, 970vs, 940w, 840s, 810m, 770m, 730w, 610m, 550w and 510w (Found: C, 38.71; H, 7.49; N, 2.16; V, 28.17. Calc. for $C_{60}H_{135}N_3O_{28}V_{10}$: C, 38.83; H, 7.33; N, 2.26; V, 27.44%).

$[(n\text{-}C_6H_{13})_4N]_3[H_3V_{10}O_{28}]$. The reaction between 10 mL of methanolic solution containing 0.26 g of $[(n\text{-}C_6H_{13})_4N]Br$ and decavanadic aqueous solution (0.004 M, 50 mL) yielded polycrystalline salts (0.25 g). ν_{max}/cm^{-1} 990s, 980vs, 940w, 840s, 810m, 780m, 720w and 600m (Found: C, 42.84; H, 8.18; N, 1.94; V, 23.98. Calc. for $C_{72}H_{159}N_3O_{28}V_{10}$: C, 42.72; H, 7.92; N, 2.08; V, 25.16%).

Crystal structure determinations

Structure determinations of **TEAh** and **TPAc** were carried out on a Siemens SMART CCD area detector system, those of the other compounds on RIGAKU AFC-5 or AFC-7 four-circle diffractometers. Selected experimental parameters and crystal data are reported in Table 1. Data were corrected for Lorentz, polarization and absorption effects. Decay corrections were not applied except for **TBAh**, during data collection of which three standard reflections showed significant decays as much as 17.9%. Each structure was solved by direct methods using the SHELXS 86[23] program and refined on F^2 using SHELXL 97.[24] Hydrogen atoms in the R_4N^+ cations were included using the riding model. For **TMAh**, **TPAv**, **TBAh** and **TBAc**, all the non-hydrogen atoms were refined with anisotropic displacement parameters. In the refinement of **TPAc**, V, O and N atoms were treated with anisotropic displacement parameters. In these five structures H atoms attached to surface O atoms of decavanadate frameworks were found from Fourier difference syntheses and their positional and isotropic displacement parameters were refined. For the other two structures protons on the decavanadate anions could not be located. In these cases protonation sites were deduced from bond valence sum calculations.[25] For the structure of **TEAh** the V and O atoms constituting the decavanadate framework were refined with anisotropic displacement parameters. For **TPAh** only V atoms were refined anisotropically.

CCDC reference number 186/2303.

See http://www.rsc.org/suppdata/dt/b0/b008128k/ for crystallographic files in .cif format.

Computational methods

The coordination number, CN, of decavanadate anions with respect to the cations was calculated as follows. The distribution of N atoms around a given anion with respect to r was determined, where r represents the distance between each N atom and its nearest O atom of the anion. Then the critical distance r_0 was determined so that no N atoms exist in the range $r_0 \le r \le r_0 + 1$ Å. The CN of the anion is defined as the number of N atoms counted up to r_0. For the dimeric structures, CN is first calculated as the number of cations surrounding a given dimer and then divided by two. The area of the Connolly surface[26] for each decavanadate anion was calculated using the Cerius[2] program.[27] A Connolly surface is the van der Waals surface of a molecule that is accessible to a solvent molecule having a non-zero radius. The surface is generated by rolling a spherical probe with a specified radius over the van der Waals surface of the molecule. We employed 1.4 Å for the probe radius. For **TPAc** and **TBAc** the surface area of the $[H_4V_{10}O_{28}]^{2-}$ anion was obtained by subtracting the area of a hypothetical dimer $([H_2V_{10}O_{28}]^{4-})_2$ from that of a trimer $([H_2V_{10}O_{28}]^{4-}\cdots[H_4V_{10}O_{28}]^{2-}\cdots[H_2V_{10}O_{28}]^{4-})$. For the other crystals containing dimers the surface area per anion was estimated as half of that calculated for the dimer. The distribution of C···O distances was obtained by measuring the distance between each C atom of the cations and its nearest O atom of the anion. The electrostatic and hydrogen bond energies of the hydrogen-bonded aggregates were calculated using the Cerius[2] program with the Dreiding force field parameter set,[28] to which a new atom type of V^{5+} was added. The atomic charges were obtained with the charge equilibration method.[29]

Results

Syntheses and crystal structures

All the crystals obtained here contain di-, tri- or tetraprotonated decavanadate anions, which exhibit various kinds of hydrogen-bonded assembly patterns. Table 2 lists the geometrical parameters of the hydrogen-bonded aggregates. The basic metal–oxygen frameworks of the $[H_nV_{10}O_{28}]^{(6-n)-}$ anions are the same as that found in $K_2Zn_2[V_{10}O_{28}]\cdot 16H_2O$.[7] Hydrogen-bond parameters are listed in Table 3. Table 4 lists the V–O–H angles in **TMAh**, **TPAc**, **TPAv**, **TBAc** and **TBAh**.

TMAh. With the $[(CH_3)_4N]^+$ cation, $[(CH_3)_4N]_4[H_2V_{10}O_{28}]\cdot 3.8H_2O$ (**TMAh**) was precipitated from aqueous solutions with the pH ranging from 3.0 to 7.0. In this study the diprotonated decavanadate anion, $[H_2V_{10}O_{28}]^{4-}$, was found solely in this $[(CH_3)_4N]^+$ salt; the larger cations precipitated triply or quadruply protonated anions. Protonation occurs at two surface O atoms, O(C1) and O(B1), bridging equatorial [V(1) or V(2)] and axial [V(3)] V atoms. These H atoms hydrogen-bond to $O(E1^I)$ and $O(G1^I)$ of an adjacent anion, to form a quadruply hydrogen-bonded centrosymmetric dimer. Fig. 2 is an ORTEP III[30] diagram showing the arrangement of the two diprotonated decavanadate anions, which is similar to that found in $[(CH_3)_4N]_4[H_2V_{10}O_{28}]\cdot CH_3CO_2H\cdot 2.8H_2$.[16] This dimer is a geometrical isomer of the $([H_2V_{10}O_{28}]^{4-})_2$ dimer found in $[(n\text{-}C_3H_7)_2NH_2]_4[H_2V_{10}O_{28}]$.[17] Comparing these two geometrical

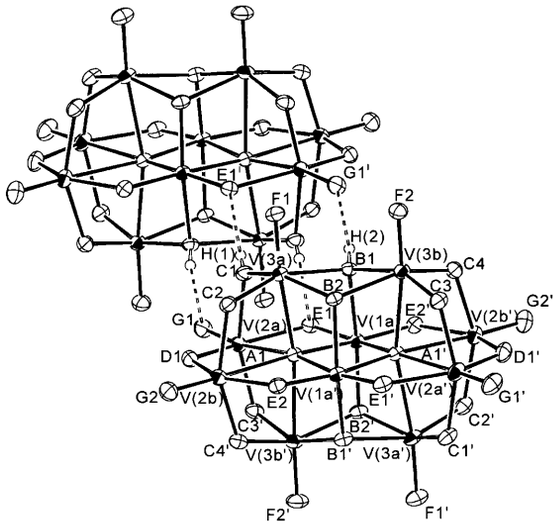

Fig. 2 ORTEP III drawing of the $([H_2V_{10}O_{28}]^{4-})_2$ dimer in **TMAh**. Hydrogen bonds connecting the two anions are shown as broken lines. For clarity, labels for the O atoms are shown without the symbol O. Displacement ellipsoids for non-H atoms are scaled to enclose 30% probability levels. Symmetry code: (I) $1 - x$, $1 - y$, $1 - z$.

isomers, the hydrogen-bond acceptor sites are different while the protonation sites are identical. Hereafter we refer to the former as a "*horizontal*" dimer and the latter as a "*vertical*" one because the arrangement of the two anions is nearly parallel and perpendicular to the equatorial planes of the anions, respectively. The geometry of the diprotonated horizontal dimer resembles that of the $([H_3V_{10}O_{28}]^{3-})_2$ dimer found in its $[(C_6H_5)_4P]^+$ salt,[5] but differs in the number of hydrogen bonds connecting the two decavanadate units as a direct consequence of the degree of protonation. One water molecule, labeled as OW3A, has short contacts to two $([H_2V_{10}O_{28}]^{4-})_2$ dimers, resulting in an infinite zigzag chain structure along the crystallographic *a* axis. The chains are separated from each other by the surrounding $[(CH_3)_4N]^+$ cations and no interactions between the chains are observed. The hydrogen-bonded zigzag chain is quite similar to that found in $[(CH_3)_4N]_4[H_2V_{10}O_{28}]\cdot CH_3CO_2H\cdot 2.8H_2O$.[16] In **TMAh** the space occupied by acetic acid is filled by two water molecules labeled as OW2A, OW2B, OW4A and OW4B, which are severely disordered.

TEAh. With the $[(C_2H_5)_4N]^+$ cation, $[(C_2H_5)_4N]_3[H_3V_{10}O_{28}]\cdot 2H_2O$ (**TEAh**) was obtained from the solutions with the pH from 3.0 to 6.0. The bond valence sum (BVS) values for O atoms of the decavanadate anion range from 1.85 to 2.27, with the exception of O(C1), O(B1) and O(C4) which show BVS values from 1.24 to 1.31, suggesting that they are protonated. These protonated O atoms are hydrogen-bonded to O(E2′^{I}), O(E1^{I}) and O(G1^{I}) atoms of a symmetry related anion to form a sextuply hydrogen-bonded centrosymmetric dimer, the configuration of which is identical with that found in the $[(C_6H_5)_4P]^+$ salt.[5] Just like the diprotonated dimers, we refer to this configuration as "horizontal". Water molecules, labeled as O(W1A), O(W1B) and O(W2), hydrogen-bond to terminal O(F1′) and O(F2′) atoms [O(W1A)···O(F1′) 2.99(2), O(W1B)···O(F1′) 2.88(2) and O(W2B)···O(F2′) 2.93(2) Å]. There are no interactions between the dimers, which are separated from each other by the $[(C_2H_5)_4N]^+$ cations. The large atomic displacement parameters of the C atoms of the cations, as well as the fact that three of the four independent $[(C_2H_5)_4N]^+$ cations are severely disordered, suggest that the $[(C_2H_5)_4N]^+$ cation has insufficient volume completely to fill the void space among the anions in this crystal.

TPAh. $[(n\text{-}C_3H_7)_4N]_3[H_3V_{10}O_{28}]\cdot 0.5H_2O$ (**TPAh**) was obtained from aqueous solutions with the pH ranging from 5.0 to 6.0

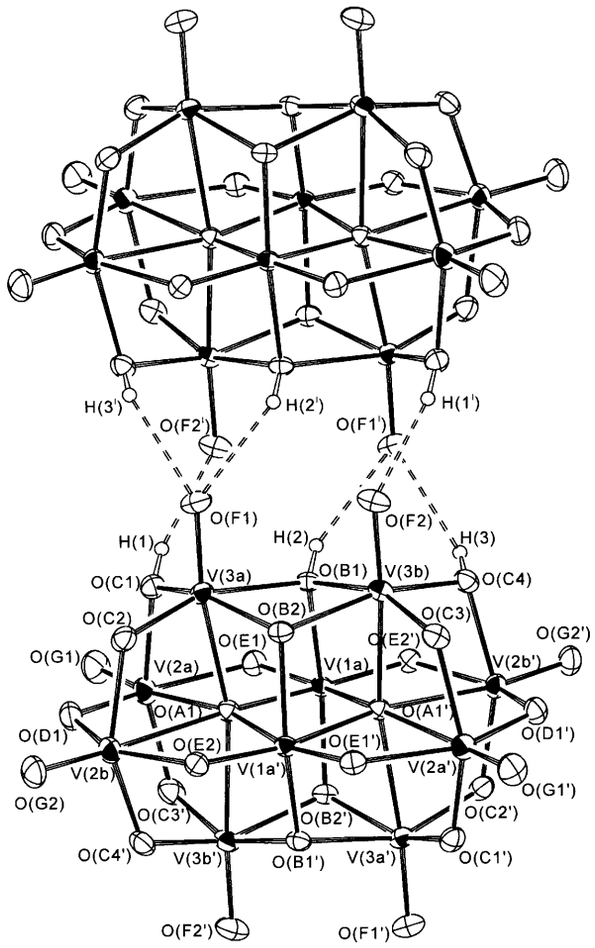

Fig. 3 ORTEP III drawing of the vertical $([H_3V_{10}O_{28}]^{3-})_2$ dimer in **TPAv**. Hydrogen bonds connecting the two anions are shown as broken lines. Displacement ellipsoids and symmetry code as in Fig. 2.

when the molar ratio of decavanadate anions to $[(n\text{-}C_3H_7)_4N]^+$ cations was larger than 3.3. At first the structure was solved in the centrosymmetric space group *C*2/*c*, in which one of the three cations was disordered between two positions with the central N atoms 3.5 Å apart. A more reasonable model was obtained in the space group *Cc*, which was finally employed. The asymmetric unit includes six $[(n\text{-}C_3H_7)_4N]^+$ cations, one water molecule and two independent triprotonated anions (anions A and B). The two anions and two pairs of cations are almost symmetrical with respect to the inversion center that disappears upon lowering the space group symmetry from *C*2/*c* to *Cc*. The remaining two cations and a water molecule are responsible for the lowering of the symmetry. The BVS values of O(C4A), O(B1A), O(C1A), O(C4B), O(B1B) and O(C1B) ranging from 1.20 to 1.32 indicate that they are protonated. These O atoms are hydrogen-bonded to O(G1B), O(E1B), O(E2′B), O(G1A), O(E1A) and O(E2′A) to form a horizontal dimer. The water molecule O(W1) is located on one side of the dimer and is weakly hydrogen-bonded to O(D1B) and O(G2′A) atoms.

TPAv. $[(n\text{-}C_3H_7)_4N]_3[H_3V_{10}O_{28}]$ (**TPAv**) was obtained from aqueous solutions with the pH ranging from 5.0 to 6.0 and with the molar ratio of decavanadate anions to $[(n\text{-}C_3H_7)_4N]^+$ cations less than 0.17. Note that **TPAv** precipitates under cation-rich conditions, **TPAh** under anion-rich conditions. Although the protonation sites of the anion are identical with those in **TEAh** and **TPAh**, the hydrogen bond acceptor sites are different. In **TPAv** two axial terminal O atoms, O(F1) and O(F2), accept hydrogen bonds. Consequently, two anions form a different type of dimer from the horizontal one. As is shown in Fig. 3, two anions of this dimer approach each other from "vertical"

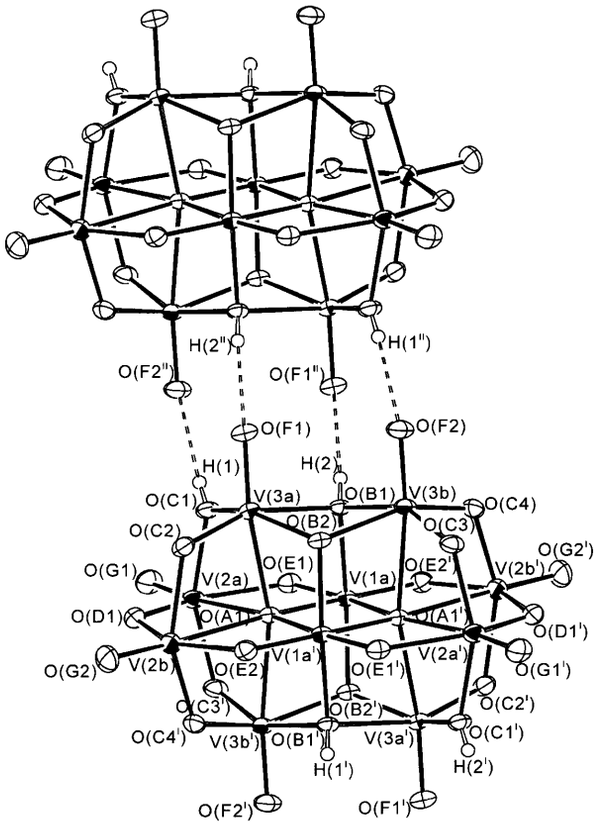

Fig. 4 ORTEP III drawing of the $([H_4V_{10}O_{28}]^{2-})_\infty$ polymer in **TPAc**. Symmetry code: (II) $-x$, $1-y$, $1-z$. Other details as in Fig. 3.

directions. This is the first example of a vertical dimer of the triprotonated decavanadate anions, and the arrangement resembles that of the diprotonated vertical dimer observed in $[(n\text{-}C_3H_7)_2NH_2]_4[H_2V_{10}O_{28}]$[17] and the chain structure of $([H_4V_{10}O_{28}]^{2-})_\infty$ observed in **TPAc** and **TBAc**. The excess of hydrogen-bond donors over hydrogen-bond acceptors results in multicenter hydrogen bonds in which an O atom accepts two hydrogen bonds. The O···O distances for these two hydrogen bonds [2.893(3) and 2.961(3) Å] are significantly longer than the others [2.702(4) to 2.812(5) Å]. In contrast to **TPAh**, no water molecules are included in the structure. The displacement parameters of the C and N atoms in the $[(n\text{-}C_3H_7)_4N]^+$ cations are smaller than in **TPAh**.

TPAc. With the $[(n\text{-}C_3H_7)_4N]^+$ cation, $[(n\text{-}C_3H_7)_4N]_2[H_4V_{10}O_{28}]$ (**TPAc**) was obtained with the pH ranging from 3.0 to 4.5, regardless of the molar ratio of the cations to the anions. The tetraprotonated anion is located on an inversion center. Protons are attached to O(C1), O(B1) and their symmetry related atoms, $O(C1^I)$ and $O(B1^I)$. Protonated O atoms are hydrogen-bonded to terminal $O(F1^{II})$ and $O(F2^{II})$ atoms belonging to adjacent decavanadate anions to from a quadruply hydrogen-bonded chain structure, as shown in Fig. 4. The configuration of this chain is the same as that found in $[(n\text{-}C_4H_9)_4N]_2[H_4V_{10}O_{28}]$.[20] The hydrogen-bonded chains are separated from each other by $[(n\text{-}C_3H_7)_4N]^+$ cations and no interactions are observed between the chains.

TBAh. With the $[(n\text{-}C_4H_9)_4N]^+$ cation, $[(n\text{-}C_4H_9)_4N]_3[H_3V_{10}O_{28}]$ (**TBAh**) was obtained in the pH range from 4.5 to 6.0. It consists of three independent $[(n\text{-}C_4H_9)_4N]^+$ cations and a triprotonated anion $[H_3V_{10}O_{28}]^{3-}$. Two anions form a horizontal dimer with the structure shown in Fig. 5. The dimers are separated from each other by $[(n\text{-}C_4H_9)_4N]^+$ cations and no interactions are observed between them.

TBAc. With the $[(n\text{-}C_4H_9)_4N]^+$ cation, $[(n\text{-}C_4H_9)_4N]_2[H_4V_{10}O_{28}]$ (**TBAc**) was obtained in the pH range from 3.0 to 4.5. The structure of this compound had been reported by Wang *et al.*,[20] but its redetermination in the present study clarified the positions of the protons and details of the hydrogen bond geometries. As predicted by Wang *et. al.* protonation occurs at O(C1), O(B1) and their symmetry-related atoms, $O(C1^I)$ and $O(B1^I)$. These O atoms form hydrogen bonds to O(F1) and O(F2) atoms of adjacent anions to construct a chain structure, $([H_4V_{10}O_{28}]^{2-})_\infty$.

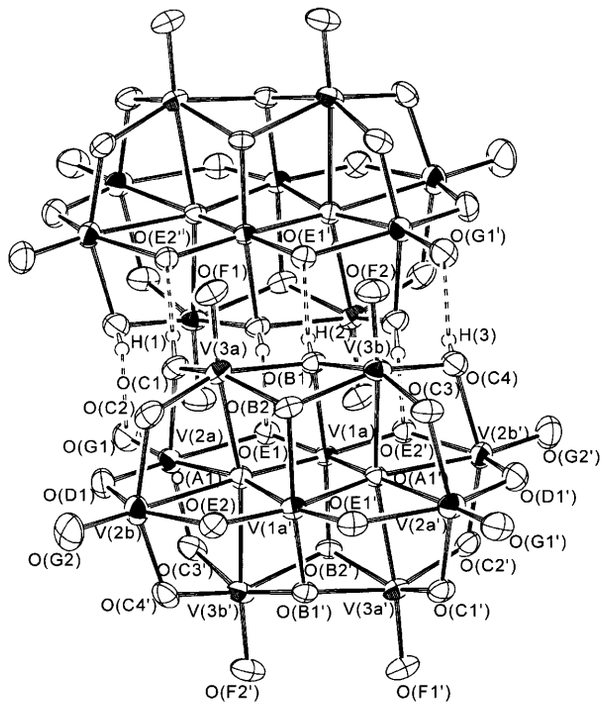

Fig. 5 ORTEP III drawing of the horizontal $([H_3V_{10}O_{28}]^{3-})_2$ dimer in **TBAh**. Details as in Fig. 3.

Infrared spectra

Fig. 6 shows the IR spectra of four tetraalkylammonium decavanadate salts containing different types of hydrogen-bonded aggregates. The extent of the splitting of the band at around 950 cm^{-1}, which is assigned to the terminal V=O stretching mode, correlates with the number of hydrogen bonds in which terminal O atoms are involved. This splitting arises from the following two effects. First, protonation to a bridging O atom elongates the V–O(H) bond and then shortens its neighboring terminal V=O bonds, which results in increased frequencies for the terminal V=O stretching mode.[14,31] Secondly, hydrogen bonds to the terminal O atoms reduce the force constants of the V=O bonds. Although a more detailed interpretation of the whole spectra is difficult, these spectra can be used as fingerprints for distinguishing the four assembly patterns of protonated decavanadate anions. Thus, since the IR spectra of the $[(n\text{-}C_5H_{11})_4N]_3[H_3V_{10}O_{28}]$ and $[(n\text{-}C_6H_{13})_4N]_3[H_3V_{10}O_{28}]$ salts resemble those of **TEAh**, **TPAh**, and **TBAh**, we expect that they contain triprotonated horizontal dimers.

Discussion

Protonation

Our crystal structure analyses of seven crystals containing various hydrogen-bonded aggregates of protonated decavanadate anions have revealed their protonation sites and hydrogen-bond acceptor sites. Di- and tri-protonated anions form dimers whereas tetraprotonated anions form chain structures. This explains the fact that tetraprotonated species, for which the hydrogen-bonded chain structures imply low solubility, are not

Table 1 Crystal data and experimental conditions

	TMAh	TEAh	TPAc	TPAh	TPAv	TBAc	TBAh
Chemical formula	$C_{16}H_{57.6}N_4O_{31.8}V_{10}$	$C_{24}H_{67}N_3O_{30}V_{10}$	$C_{24}H_{60}N_2O_{28}V_{10}$	$C_{36}H_{88}N_3O_{28.5}V_{10}$	$C_{36}H_{87}N_3O_{28}V_{10}$	$C_{32}H_{76}N_2O_{28}V_{10}$	$C_{48}H_{111}N_3O_{28}V_{10}$
Formula weight	1324.55	1387.21	1334.14	1528.49	1519.49	1446.35	1687.80
Crystal system	Triclinic	Monoclinic	Monoclinic	Monoclinic	Monoclinic	Monoclinic	Triclinic
Space group (no.)	$P\bar{1}$ (2)	$C2/c$ (15)	$P2_1/n$ (14)	Cc (9)	$P2_1/c$ (14)	$P2_1/n$ (14)	$P\bar{1}$ (2)
a/Å	12.645(3)	33.4919(9)	8.5568(1)	27.994(4)	20.303(1)	8.5633(9)	15.968(2)
b/Å	15.695(4)	21.5128(5)	13.1873(2)	24.643(4)	14.010(1)	21.048(3)	18.677(2)
c/Å	12.627(3)	13.9059(4)	20.1901(3)	17.905(2)	21.991(2)	15.435(2)	12.785(2)
α/°	96.71(2)						91.38(1)
β/°	101.24(2)	98.552(1)	92.653(1)	95.448(9)	110.996(5)	96.38(1)	96.48(1)
γ/°	68.14(2)						107.26(1)
V/Å^3	2278(1)	9907.9(5)	2275.82(8)	12296(3)	5839.7(8)	2764.9(6)	3611.1(8)
Z	2	8	2	8	4	2	2
T/K	298	298	298	298	298	298	298
μ(Mo-Kα)/mm^{-1}	2.05	1.89	2.04	1.53	1.61	1.69	1.31
Number of measured/independent reflections	10961/10486	39819/12329	16898/5664	16466/8347	13743/13371	6330/6330	17185/16587
R_{int}	0.035	0.077	0.060	0.086	0.038	N/A	0.041
$R1(F_0)$ for observed data/$wR2(F_0^2)$ for all data	0.048/0.148	0.059/0.198	0.047/0.120	0.057/0.197	0.042/0.115	0.039/0.136	0.054/0.268

Table 2 Configurations of the hydrogen-bonded aggregates[a]

Compound	X[b]/Å	Y/Å	Z/Å	r[c]/Å
TMAh	−4.6174	6.3996	3.4120	8.598
TEAh	−1.2599	6.3879	3.5204	7.402
TPAh	−1.2710	6.4642	3.3350	7.384
TBAh	−1.8940	6.5319	3.1583	7.499
TPAv	−0.2799	3.4587	7.5705	8.328
TPAc	−1.9397	3.3792	7.6268	8.564
TBAc	−1.8869	3.4913	7.5880	8.563

[a] For each aggregate, the coordinate of the center of gravity of an anion with respect the coordinate system fixed to its hydrogen-bonded pair is listed. [b] The coordinate system is defined in Fig. 1. [c] $r = (X^2 + Y^2 + Z^2)^{1/2}$.

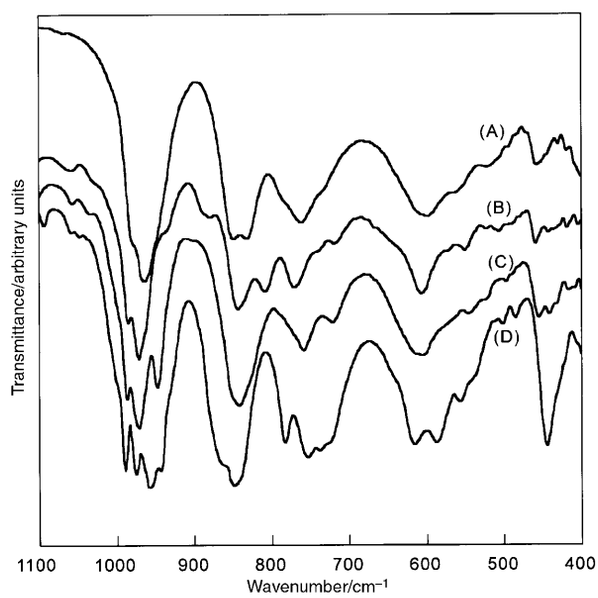

Fig. 6 Infrared absorption spectra of (A) **TMAh**, (B) **TPAh**, (C) **TPAv**, and (D) **TPAc**.

observed in aqueous solutions.[8] Protonation occurs at some of the O(B) and O(C) atoms bridging equatorial and axial vanadium atoms, in agreement with the results hitherto reported.[5,11,12,17,20] Other surface O atoms, with the exception of O(D), accept hydrogen bonds. With the $[(n\text{-}C_3H_7)_4N]^+$ cation, **TPAc** was obtained from aqueous solutions with pH from 3.0 to 4.5, and either **TPAh** or **TPAv** from pH 4.5 to 6.0. With the $[(n\text{-}C_4H_9)_4N]^+$ cation, **TBAc** precipitated from solutions with pH ranging from 3.0 to 4.5 and **TBAh** from pH 4.5 to 6.0. It is a significant feature, found only when using the $[(n\text{-}C_3H_7)_4N]^+$ and $[(n\text{-}C_4H_9)_4N]^+$ cations, that the degree of protonation depends on the acidity of the mother liquor. On the contrary, each of the other cations, R_4N^+ where R = CH_3, C_2H_5, n-C_5H_{11} or n-C_6H_{13}, gave only one particular aggregation pattern. These results indicate that the decavanadate anion in each protonation step has some effective packing patterns that can be achieved only with some specific cations. The numbers of water molecules of crystallization are 3.8 in **TMAh**, 2 in **TEAh**, 0.5 in **TPAh**, and zero in the other structures. $[(n\text{-}C_3H_7)_4N]^+$ and $[(n\text{-}C_4H_9)_4N]^+$ cations are exceptional in that they are suitable for both tri- and tetra-protonated decavanadate anions to form effective packing arrangements with little or no void spaces to be filled by water molecules of crystallization.

In aqueous solution, protonation of the decavanadate anions proceeds according to the decrease in the pH of the solution.[8] However, the pH of the mother liquor is not the only factor determining the degree of protonation in the crystals. The degree of protonation changes systematically from H_2 to H_4 as the size of the cation becomes larger from $[(CH_3)_4N]^+$ to

Table 3 Hydrogen bond geometries in the seven decavanadate crystals

Compound		D–H/Å	H···A/Å	D···A/Å	D–H···A/°	A···D–H/°
TMAh	O(C1)–H(1)···O(E1^{I})	0.57(4)	2.19(5)	2.763(5)	176(7)	3(5)
	O(B1)–H(2)···O(G1^{I})	0.72(5)	2.06(5)	2.766(5)	169(5)	8(4)
TEAh	O(C4)···O(G1^{I})			2.758(5)		
	O(B1)···O(E1^{I})			2.764(4)		
	O(C1)···O(E2′^{I})			2.764(4)		
TPAh	O(C4A)···O(G1B)			2.71(2)		
	O(B1A)···O(E1B)			2.79(3)		
	O(C1A)···O(E2′B)			2.72(3)		
	O(C4B)···O(G1A)			2.77(2)		
	O(B1B)···O(E1A)			2.72(3)		
	O(C1B)···O(E2′A)			2.76(2)		
TBAh	O(C4)–H(3)···O(G1^{I})	0.62(5)	2.16(5)	2.759(6)	165(7)	12(5)
	O(B1)–H(2)···O(E1^{I})	0.68(5)	2.14(5)	2.812(5)	168(6)	9(5)
	O(C1)–H(1)···O(E2′^{I})	0.76(6)	2.03(6)	2.783(5)	174(6)	5(4)
TPAv	O(C1)–H(1)···O(F2^{I})	0.75(4)	2.06(4)	2.787(3)	162(4)	13(3)
	O(B1)–H(2)···O(F1^{I})	0.71(3)	2.24(3)	2.893(3)	153(4)	21(3)
	O(C4)–H(3)···O(F1^{I})	0.67(3)	2.34(3)	2.961(3)	155(4)	19(3)
TPAc	O(B1)–H(2)···O(F1^{II})	0.75(4)	1.98(5)	2.702(4)	161(5)	14(3)
	O(C1)–H(1)···O(F2^{II})	0.66(5)	2.06(5)	2.717(4)	174(7)	5(5)
TBAc	O(B1)–H(2)···O(F1^{III})	0.74(4)	2.01(4)	2.725(3)	162(4)	13(3)
	O(C1)–H(1)···O(F2^{III})	0.48(5)	2.29(5)	2.742(4)	160(8)	17(7)

Symmetry codes: (I) $1 - x$ and, $1 - y$, $1 - z$; (II) $-x$, $1 - y$, $1 - z$; (III) $2 - x$, $1 - y$, $1 - z$.

Table 4 V–O–H bond angles (°) in selected decavanadate crystals

Compound	V(1)–O(B)–H		V(3)–O(B)–H		V(2)–O(C)–H		V(3)–O(C)–H	
TMAh	V(1a)–O(B1)–H(2)	109(4)	V(3a)–O(B1)–H(2)	115(4)	V(2a)–O(C1)–H(1)	120(5)	V(3a)–O(C1)–H(1)	126(5)
			V(3b)–O(B1)–H(2)	122(4)				
TBAh	V(1a)–O(B1)–H(2)	101(5)	V(3b)–O(B1)–H(2)	139(5)	V(2b′)–O(C4)–H(3)	109(5)	V(3b)–O(C4)–H(3)	111(5)
			V(3a)–O(B1)–H(2)	107(5)	V(2a)–O(C1)–H(1)	116(4)	V(3a)–O(C1)–H(1)	128(4)
TPAv	V(1a)–O(B1)–H(2)	120(3)	V(3b)–O(B1)–H(2)	110(3)	V(2b′)–O(C4)–H(3)	117(3)	V(3b)–O(C4)–H(3)	112(3)
			V(3a)–O(B1)–H(2)	118(3)	V(2a)–O(C1)–H(1)	125(3)	V(3a)–O(C1)–H(1)	112(3)
TPAc	V(1a)–O(B1)–H(2)	114(3)	V(3a)–O(B1)–H(2)	111(3)	V(2a)–O(C1)–H(1)	125(5)	V(3a)–O(C1)–H(1)	122(5)
			V(3b)–O(B1)–H(2)	118(3)				
TBAc	V(1a)–O(B1)–H(2)	120(3)	V(3a)–O(B1)–H(2)	118(3)	V(2a)–O(C1)–H(1)	114(7)	V(3a)–O(C1)–H(1)	131(7)
			V(3b)–O(B1)–H(2)	107(3)				

Table 5 CNs, Connolly surface areas and distribution of C···O distances in the seven decavanadate crystals

Compound	Number of protons	Aggregation type	CN	r_0/Å	Connolly surface area[a]/Å^2	C···O distances/Å		
						mean	min.	max.
TMAh	2	Horizontal dimer	11	5.2	312.52 (312.52)	3.38(7)	3.283	3.556
TEAh	3	Horizontal dimer	7	4.5	(298.62)	3.41(20)	2.974	3.940
TPAh	3	Horizontal dimer	6.5	4.7	(295.74)	3.94(80)	3.032	6.512
TBAh	3	Horizontal dimer	6	4.5	300.44 (300.61)	3.60(34)	2.938	4.517
TPAv	3	Vertical dimer	8	4.8	307.03 (307.81)	3.46(21)	3.079	4.043
TPAc	4	Polymer	8	5.1	289.14 (290.11)	3.46(17)	3.131	3.757
TBAc	4	Polymer	6	4.8	288.98 (288.43)	3.44(14)	3.232	3.685

[a] The values in parentheses are those calculated by disregarding the H atoms.

$[(n\text{-}C_4H_9)_4N]^+$. Table 5 shows the coordination numbers and the Connolly surface areas of hydrogen-bonded anions in these crystals. The Connolly surface areas of the hydrogen-bonded aggregates decrease as the protonation proceeds. Larger cations do not allow large coordination numbers around an anion and they cannot access close to the anions, which should result in a smaller Madelung energy for these crystals. Therefore, large cations prefer highly protonated anions that can stabilize themselves by protonating and forming hydrogen-bonded aggregates, such that the disadvantage in the Madelung energy is compensated by the energy associated with the protonation and the formation of hydrogen-bonded aggregates. The anions with more protons require less cations, which is compatible with the fact that the coordination number of large cations around an anion should be small. On the other hand, a larger coordination number around an anion is possible with smaller cations, which can also approach close to the anions. Therefore, it may be more advantageous for small cations to form crystals with less protonated anions to achieve larger Madelung energy than to crystallize with more protonated anions, even if the stabilization energy upon forming aggregates is not enough for these less protonated anions. For these reasons, the larger cations tend to crystallize with highly protonated anions, whereas the smaller cations prefer less protonated anions.

Horizontal dimer and vertical dimer

There are two types of triprotonated dimeric structures: horizontal and vertical dimers. The former exists in **TEAh**, **TPAh**, **TBAh**, and probably also in the $[(n\text{-}C_5H_{11})_4N]^+$ and $[(n\text{-}C_6H_{13})_4N]^+$ salts. The latter type, which was obtained in this work

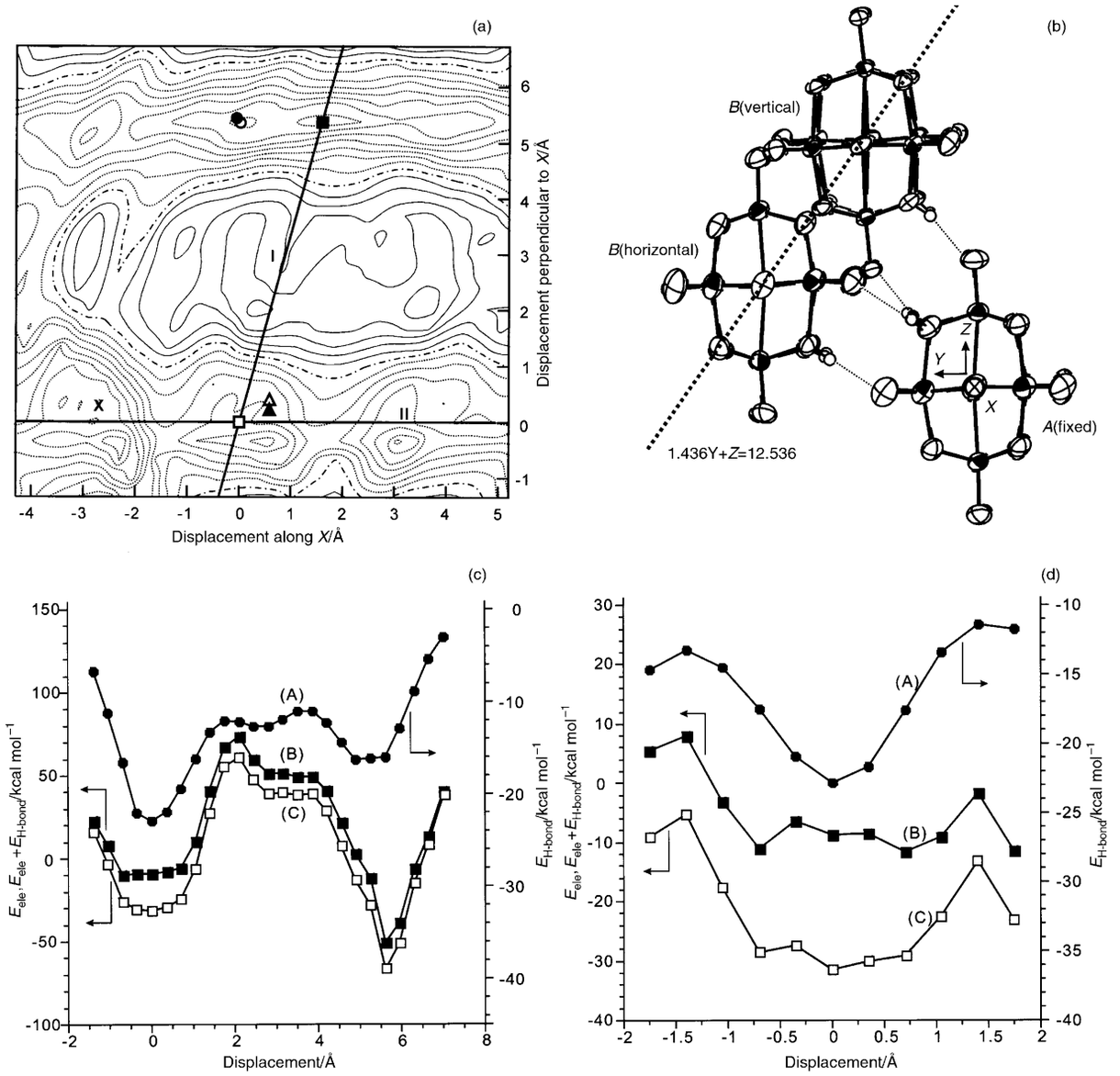

Fig. 7 (*a*) The stabilization energies of triprotonated decavanadate dimers calculated as the sum of hydrogen-bond and electrostatic potential energies. The horizontal dimer in **TBAh** and the vertical dimer in **TPAv** are superimposed so that the coordinate systems fixed to one of the pair, A, coincide as shown in (*b*). The energies are calculated by moving the other anion, B, on the plane that includes the two geometries of **TBAh** and **TPAv** and is parallel to the axis X fixed to the anion A, which is defined as $1.436Y + Z = 12.536$. The origin of this map is set to the geometry of **TBAh** and the horizontal axis is set parallel to the X axis fixed to the anion A. The contour interval is 10 kcal mol^{-1}, with negative contours broken, zero contour dot-dashed and positive contours solid. The geometries of the hydrogen-bonded aggregates are depicted as follows: (×)**TMAh**, (△)**TEAh**, (▲)**TPAh**, (□)**TBAh**, (■)**TPAv**, (●)**TPAc** and (○)**TBAc**. (*c*) The cross section along the line I in (a) that passes through the geometries of **TBAh** and **TPAv**, showing (A) hydrogen bond energies, (B) electrostatic potential energy, and (C) the sum of (A) and (B). (*d*) The cross section along line II in (a) that passes through the geometry of **TBAh** and is parallel to the X axis of the anion A, showing (A) hydrogen bond energies, (B) electrostatic potential energy, and (C) the sum of (A) and (B).

for the first time in **TPAv**, selectively precipitates from solution when the molar ratio of the $[(n\text{-}C_3H_7)_4N]^+$ cation to the $[V_{10}O_{28}]^{6-}$ anion is more than 6.0 : 1. When this ratio is less than 0.3 : 1 only **TPAh** precipitates. To estimate the stabilization energy of aggregation, we have calculated the electrostatic and hydrogen bond energies of dimers with geometries identical to and close to those of the dimers observed in the crystals. The result, shown in Fig. 7, illustrates that the horizontal and vertical dimers observed in the crystalline state are close to the energy minima, which supports our approach for estimating the aggregation energy. With respect to the coulombic interactions, the vertical dimer is more favorable. On the other hand, the stabilization of the horizontal dimer is dominated by the hydrogen bonds.

Comparison of the coordination number and the statistics of C···O distances in Table 5 illustrates that **TPAv** has more effective packing between anions and cations than **TPAh**, which results in the larger Madelung energy for the crystal of **TPAv**. Even from the solution with the cation to anion ratio suitable for **TPAh**, **TPAv** precipitates afterwards. This indicates that **TPAv** is the thermodynamically stable form and **TPAh** is a kinetically controlled product. Thus, **TPAh**, which has a smaller coordination number in the solid state, crystallizes more readily than **TPAv** only when the number of cations is extremely deficient compared with that of anions. This assertion is consistent with the suggestion that the horizontal dimer is stabilized mainly by hydrogen bonds, which may also exist in the solutions.

In order to assess the possibility that the diprotonated anions form a vertical dimer as well as the horizontal dimer, we carried out a similar calculation using the coordinates of **TMAh** and **TBAc**. The results are almost the same as for the triprotonated dimer. The structures of both the vertical and horizontal dimers correspond to energy minima and they have almost the same

area of Connolly surface (312.77 Å² for the horizontal one and 312.52 Å² for the vertical one). Although a tetraalkylammonium salt containing the vertical dimer has not been obtained so far, its dipropylammonium salt has been reported.[17]

Geometrical deviation of the dimers and the crystal packing

On closer inspection, the horizontal dimers observed in **TEAh**, **TPAh** and **TBAh** can be classified into two groups as shown in Table 2. The displacement of the two anions of the dimer in **TBAh** along the *X* axis is larger by about 0.63 Å than those in **TEAh** and **TPAh**. We call the former type Y and the latter type X. The energy curve in Fig. 7(a) indicates that the geometry of the horizontal dimers can deviate along the *X* axis from the most stable position with little change of energy. As shown in Table 4, the O–H groups display various geometries with respect to the decavanadate framework. There is a significant difference in the V–O(C)–H angles and hydrogen bond parameters between **TPAc** and **TBAc**, both of which exhibit the same hydrogen-bonded aggregation pattern. Compared with **TPAc**, the hydrogen-bonded anions in **TBAc** deviate from each other along the *Y* direction by 0.11 Å. The difference in O–H geometries between the two crystals results from the difference in configurations of hydrogen-bonded anions. The aggregation energy, estimated as the sum of the electrostatic and hydrogen bond energies for the $([H_4V_{10}O_{28}]^{2-})_2$ dimers, indicates that the aggregate in **TPAc** is less stable than that in **TBAc**. Comparison of the coordination numbers, however, shows that **TPAc** has a more effective packing between anions and cations. The difference of O–H geometries is enforced by the different packing patterns between anions and cations. From an alternative point of view, we may conclude that the geometrical tolerance of the O–H group allows some flexibility in the packing patterns adopted.

Crystal structures with the same stoichiometric index

TPAc and **TBAc** have the same A_2X stoichiometric index, where A designates a cation and X refers to an anion. **TEAh**, **TPAh** and **TBAh** have the index A_3X. Although the A_2X crystals include a common hydrogen-bonding pattern, we should regard **TPAc** and **TBAc** as different structures since they show different CNs. It is noteworthy that the structures of **TPAc** and **TBAc** correspond to a transition of structure type, analogous to that observed in simple inorganic compounds such as fluorite type ZrO_2 to cadmium iodide type ZrS_2. Also, the three A_3X crystals show structural transitions where CN decreases as the size of the R_4N^+ cation increases.

Conclusion

In this study we have demonstrated that tetraalkylammonium cations can be utilized to construct hydrogen-bonded aggregates of protonated decavanadate anions, and probably of any kind of protonated anions. Six kinds of cations gave four different types of hydrogen-bonded self-assemblies, of which the vertical triprotonated dimer shows an unprecedented configuration. The degree of protonation in the crystalline state is primarily governed by the size of the counter cations, unlike the situation in the solution state where protonation proceeds in accord with the decrease in the pH. Larger cations prefer highly protonated anions and smaller cations less protonated anions. The aggregate formation energy may be estimated quantitatively as the sum of the hydrogen-bond energies and electrostatic interactions.

Acknowledgements

The authors thank Professors T. Yashima and T. Komatsu for use of the ICP spectrometer. Thanks are also due to Dr T. Yamane for helpful discussions on the molecular dynamics calculations. This work was supported in part by a Grant in Aid for Scientific Research from the Ministry of Education, Science, Sports and Culture.

References

1 M. T. Pope, *Heteropoly and Isopoly Oxometalates*, Springer, New York, 1983.
2 C. L. Hill, ed., *Polyoxometalates*, *Chem. Rev.*, 1998, **98**, 1.
3 G. R. Desiraju, *Crystal Engineering: The Design of Organic Solids*, Elsevier, Amsterdam, 1989; *The Crystal as a Supramolecular Entity: Perspectives in Supramolecular Chemistry Vol. 2*, ed. G. R. Desiraju, Wiley, Chichester, 1996.
4 G. R. Desiraju, *Angew. Chem.*, *Int. Ed. Engl.*, 1995, **34**, 2311.
5 V. W. Day, W. G. Klemperer and D. J. Maltbie, *J. Am. Chem. Soc.*, 1987, **109**, 2991.
6 R. Mattes and K.-L. Richter, *Z. Naturforsch.*, *Teil B*, 1982, **37**, 1241; M. I. Khan, J. Zubieta and P. Toscano, *Inorg. Chim. Acta*, 1992, **193**, 17; M. I. Khan, J. Zubieta and P. Toscano, *Inorg. Chim. Acta*, 1992, **193**, 17; T. Ozeki, T. Yamase, H. Naruke and Y. Sasaki, *Bull. Chem. Soc. Jpn.*, 1994, **67**, 3249; S. Golhen, L. Ouahab, D. Grandjean and P. Molinie, *Inorg. Chem.*, 1998, **37**, 1499.
7 H. T. Evans, Jr., *Inorg. Chem.*, 1966, **5**, 967.
8 F. J. C. Rossotti and H. Rossotti, *Acta Chem. Scand.*, 1956, **10**, 957; L. Pettersson, B. Hedman, I. Andersson and N. Ingri, *Chem. Scr.*, 1983, **22**, 254; L. Pettersson, I. Andersson and B. Hedman, *Chem. Scr.*, 1985, **25**, 309.
9 O. W. Howarth and M. Jarrold, *J. Chem. Soc.*, *Dalton Trans.*, 1978, 503; W. G. Klemperer and W. Shum, *J. Am. Chem. Soc.*, 1977, **99**, 3544.
10 G. Rigotti, B. E. Rivero and E. E. Castellano, *Acta Crystallogr.*, *Sect. C*, 1987, **43**, 197.
11 P. Román, A. Aranzabe, A. Luque, J. M. Gutiérrez-Zorrilla and M. Martínez-Ripoll, *J. Chem. Soc.*, *Dalton Trans.*, 1995, 2225.
12 M. Farahbakhsh, P. Kögerler, H. Schmidt and D. Rehder, *Inorg. Chem. Commun.*, 1998, **1**, 111.
13 M. Shao, L. Wang, Z. Zhang and Y. Tang, *Sci. Sinica*, 1984, **B27**, 137; M. V. Capparelli, D. M. L. Goodgame, P. B. Hayman and A. C. Skapski, *J. Chem. Soc.*, *Chem. Commun.*, 1986, 776; M. Farahbakhsh, H. Schmidt and D. Rehder, *Chem. Ber.*, 1997, **130**, 1123; T. Debaerdemaeker, J. M. Arrieta and J. M. Amigo, *Acta Crystallogr.*, *Sect. B*, 1982, **38**, 2465; D. Riou, O. Roubeau and G. Férey, *Z. Anorg. Allg. Chem.*, 1998, **624**, 1021.
14 A. S. J. Wery, J. M. Gutierrez-Zorrila, A. Luque and P. Roman, *Polyhedron*, 1996, **15**, 4555.
15 J. M. Arrieta, *Polyhedron*, 1992, **11**, 3045.
16 B. Pecquenard, P. Y. Zavalij and M. S. Whittingham, *Acta Crystallogr.*, *Sect. C*, 1998, **54**, 1833.
17 A. E. Lapshin, Yu. I. Smolin, Yu. F. Shepelev, L. Zhurkova and D. Depesheva, *Kristallografiya*, 1997, **42**, 677.
18 J. M. Arrieta, A. Arnaiz, L. Lorente, C. Santiago and G. Germain, *Acta Crystallogr.*, *Sect. C*, 1988, **44**, 1004.
19 C. Santiago, A. Arnaiz, L. Lorente, J. M. Arrieta and G. Germain, *Acta Crystallogr.*, *Sect. C*, 1988, **44**, 239.
20 W. Wang, F. Zeng, X. Wang and M. Tan, *Polyhedron*, 1996, **15**, 265.
21 Throughout this paper, the atom type notation given by Day *et al.*,[5] which is illustrated in Fig. 1, is employed.
22 K. F. Jahr and F. Preuss, *Chem. Ber.*, 1965, **98**, 3297.
23 G. M. Sheldrick, SHELXS 86, Program for the Solution of Crystal Structures, University of Göttingen, 1985.
24 G. M. Sheldrick, SHELXL 97, Program for the Refinement of Crystal Structures, University of Göttingen, 1997.
25 D. Altermatt and I. D. Brown, *Acta Crystallogr.*, *Sect. B*, 1985, **41**, 240.
26 M. L. Connolly, *J. Appl. Crystallogr.*, 1983, **16**, 548.
27 Cerius², release 3.0, Molecular Simulation Inc., Burlington, MA, 1997.
28 S. L. Mayo, B. D. Olafson and W. A. Goddard III, *J. Phys. Chem.*, 1990, **94**, 8897.
29 A. K. Rappé and W. A. Goddard III, *J. Phys. Chem.*, 1991, **95**, 3358.
30 M. N. Burnett and C. K. Johnson, ORTEP III, Report ORNL-6895, Oak Ridge National Laboratory, Oak Ridge, TN, 1996.
31 W. P. Griffith and P. J. B. Lesniak, *J. Chem. Soc. A*, 1969, 1066; F. Corigliano and S. di Pasquale, *Inorg. Chim. Acta*, 1975, **12**, 99; J. Fuchs, S. Mahjour and R. Palm, *Z. Naturforsch.*, *Teil B*, 1976, **31**, 544.